Fermi National Accelerator Laboratory

FERMILAB Conf-94/148-E
CDF

A Precision Measurement of the Prompt Photon Cross Section in $p\bar{p}$ Collisions at $\sqrt{s}$ = 1.8 TeV

The CDF Collaboration

Fermi National Accelerator Laboratory
P.O. Box 500, Batavia, Illinois 60510

June 1994

Submitted to the *27th International Conference on High Energy Physics*, Glasgow, Scotland, July 20-27, 1994

ICHEP94 Ref.
Submitted to Pa 11
Pl 13

CDF/PUB/JET/PUBLIC/2605
May 27, 1994
FERMILAB-CONF-94/148-E

A Precision Measurement of the Prompt Photon Cross Section in $p\bar{p}$ Collisions at $\sqrt{s} = 1.8$ TeV

The CDF Collaboration[1]

Abstract

A prompt photon cross section measurement from the CDF experiment at the Fermilab $p\bar{p}$ Collider is presented. Detector and trigger upgrades, as well as six times the integrated luminosity compared with our previous publication, have contributed to a much more precise measurement and extended P_T range. As before, the cross section agrees qualitatively with QCD calculations but has a steeper slope at low P_T.

[1]Contributed by Stephen E. Kuhlmann, Argonne (Internet kuhlmann@fnald.fnal.gov)
Submitted 27th International Conference on High Energy Physics, University of Glasgow, Glasgow, Scotland, July 20-27, 1994

In this letter we present a measurement of the cross section for production of isolated prompt photons in proton-antiproton collisions at $\sqrt{s} = 1.8$ TeV using the Collider Detector at Fermilab (CDF). With six times the data sample, plus detector and trigger additions, this measurement is a significant improvement over our previously published results [1]. Prompt photons are produced in the initial collision, in contrast to photons produced by decays of hadrons. In Quantum Chromodynamics (QCD), at lowest order, prompt photon production is dominated by the Compton process ($gq \rightarrow \gamma q$), which is sensitive to the gluon distribution of the proton [2]. The precision of the present measurement provides a quantitative test of QCD and parton distributions in a fractional momentum range $.013 < x < .13$.

A detailed description of the CDF detector may be found in [3], and the important components are the same as used in the previous analysis, with one addition. In order to improve the measurement systematic uncertainties, and separate signal from background at higher photon P_T, a set of multiwire proportional chambers were added in front of the central electromagnetic calorimeter (CEM). These are called the Central Preshower (CPR) chambers. These chambers sample the electromagnetic showers that begin in the solenoid magnet material(1.075 X0) in front of them. The chambers have 2.22 cm cells segmented in $r - \phi$, and are positioned at a radius of 168 cm from the beamline. There are 4 chamber divisions spanning ± 1.1 unit of pseudorapidity, η, (defined by the expression $\eta = -\ln(\tan\theta/2)$). The other important detector component used for this analysis is the Central Electromagnetic Strip (CES) chambers, used in the previously published measurement. These chambers provide the photon position measurement as well as measuring the transverse profile of the electromagnetic shower.

In addition to the detector improvement noted above, the photon hardware trigger was upgraded. The photon trigger consists of three levels. At the first level, a single tower in the CEM is required to be above a threshold, typically $P_T > 6$ GeV/c. Previously in the second trigger level the only requirement was that 89% of the photon transverse energy be in the EM compartment of the calorimeter. Additional electronics were added at this level to require that the transverse energy in the 5×5 grid of trigger towers surrounding the photon

candidate (equivalent to a radius $R = \sqrt{(\Delta\eta)^2 + (\Delta\phi)^2} = 0.65$) was less than 5 GeV, thereby requiring the photon to be *isolated.* Due to trigger rate limitations, the main photon trigger would have had a $P_T > 30$ GeV/c threshold without this isolation cut and the data from 16-30 GeV/c would have been prescaled by approximately $\times 100$. With the upgraded trigger the threshold was 16 GeV/c with no prescale. In addition, a $P_T > 6$ GeV/c prescaled trigger with the same isolation requirement was used, as well as a $P_T > 50$ GeV/c trigger without the isolation cut. In the third level of the trigger, software algorithms applied fiducial cuts to the photons and stiffened the isolation cut to 4 GeV in a cone radius of 0.7. Integrated luminosities for the 3 trigger thresholds were 19, 16, 0.05 pb^{-1} for the 50, 16, 6 GeV/c thresholds respectively, including the effect of prescales.

The selection of prompt photon candidates from the triggered events is essentially unchanged from those used previously [1], and we briefly review them here. Candidates were rejected if there was a reconstructed charged track pointing at the CPR chamber containing the photon. To improve the signal/background ratio, the isolation cut applied in the trigger was tightened to 2 GeV in a cone radius of 0.7. Cuts on the event z vertex and missing transverse energy were applied as before with slight changes [4]. At this point, the main backgrounds to the prompt photons are from single π^0 and η mesons, with smaller backgrounds from other multi-π^0 states. The single and multiple meson backgrounds are all reduced by requiring there is no other photon candidate above 1 GeV energy in the CES region corresponding to the photon's calorimeter towers. The total acceptance of prompt photons, including efficiencies for all these cuts is approximately 38% with a small P_T dependence. This is slightly smaller than our previously published acceptance due to the effect of multiple collisions at the higher luminosities.

We employ two methods for statistically subtracting the remaining neutral meson background from our photon candidates: the *conversion method* counts the fraction of photon conversions in the solenoid magnet material by using the CPR, and the *profile method* uses the transverse profile of the electromagnetic shower in the CES. For the conversion method, the probability of a single photon conversion is $\approx 60\%$, while that for the two-photon de-

cay of a π^0 or η is larger, $\approx$ 84%. For the profile method, the transverse profile of each photon candidate was compared to that measured for electrons in a test beam in the same momentum range. A measure of the goodness of fit ($\tilde{\chi}^2$ [1]) was statistically larger for a neutral meson (poor fit) than for a single photon (good fit) because a neutral meson usually produced a wider EM shower. The conversion method has the advantage of much smaller systematic uncertainties and an unlimited P_T range. But the profile method has the advantage of a better separation of signal and background than the conversion method in the low P_T region. We thus use the profile method from 10-16 GeV/c P_T and the conversion method everywhere else.

For both background subtraction methods, the number of photons (N_γ) in a bin of P_T is obtained from the number of photon candidates (N), the fraction of photon candidates that pass a fixed cut defined below (ϵ), and the corresponding fractions for true photons (ϵ_γ) and background (ϵ_b), using:

$$N_\gamma = \left(\frac{\epsilon - \epsilon_b}{\epsilon_\gamma - \epsilon_b} \right) N \tag{1}$$

Equation 1 comes from $\epsilon N = \epsilon_\gamma N_\gamma + \epsilon_b N_b$ with $N_b = N - N_\gamma$. For the conversion method, ϵ is the fraction of photon candidates which produce a pulse height of greater than 1 minimum ionizing particle in the CPR, within a 66 milliradian "window" (5 CPR channels) around the photon direction. For reference the minimum separation of the two photons from a 25 GeV/c π^0 is 11 mr. For the profile method, ϵ is the fraction of events which have $\tilde{\chi}^2 < 4$ out of all events with $\tilde{\chi}^2 < 20$. Using these methods, we measure the signal/background ratio bin-by-bin and propagate that bins' statistical uncertainty into the cross section measurement, including the effect of the background subtraction.

For the conversion method ϵ_γ is estimated from first principles using the equation: ϵ_γ = 1. - EXP(-7/9 * X0) where X0 is the amount of material in radiation lengths in front of the CPR. Corrections to this estimate of ϵ_γ are made on an event basis for the different amount of material traversed due to angular effects, as well as changes in the photon pair production cross section with photon energy. For the photon pair production cross section we use the tables in reference [5]. An additional correction is made for photon showers that

begin after the photon has passed through the CPR, but a soft photon or electron from the shower is scattered backwards at a large angle and gives a CPR signal. This correction was estimated with an electromagnetic shower simulation [6]. The final correction to ϵ_γ is due to CPR signals arising from soft photons from the underlying event. This was estimated using minimum bias triggers. The fraction of background events that give a CPR signal, ϵ_b, is the same as ϵ_γ except for the multiple photons from the background:
ϵ_b = 1. - EXP(-7/9 * X0 * $N_\gamma(P_T)$). The function $N_\gamma(P_T)$ is the average number of photons within the CPR "window" defined earlier. This changes with particle P_T and type, and is estimated using a detector simulation of π^0, η and K_S^0 mesons with a relative production ratio of 1:1:0.4 [1]. All of the corrections mentioned earlier for ϵ_γ are applied to ϵ_b as well.

For the profile method ϵ_γ and ϵ_b are the same as in reference [1]. For both methods ϵ, ϵ_γ, ϵ_b are shown in figure 1, along with ϵ for the previous measurement using only the profile method. Note that the data fractions are close to the single photon expectation at high P_T (signal/background $\approx$ 18), while they are consistent with nearly 100% background at P_T below 10 GeV/c. Due to this small signal/background ratio, cross section measurements will only be presented above 10 GeV/c at this time.

The systematic uncertainty in the prompt photon cross section is due mostly to uncertainties in ϵ_γ and ϵ_b. For both methods we can check these fractions using reconstructed π^0, η, and ρ mesons, shown in figure 2. The measured (expected) CPR conversion rate for the π^0 is $.842 \pm .008$ (.847), for the η is $.831 \pm .012$ (.842), and for the ρ is $.836 \pm .01$ (.834). The uncertainty in the expected CPR conversion rate, due to the material count for the solenoid magnet, is .006. There is excellent agreement between the measured and predicted rates in all three cases, thus we will use .006 for the uncertainty in ϵ_b. This translates into a .0078 uncertainty in ϵ_γ, and is completely correlated with the ϵ_b uncertainty. These uncertainties combined lead to a 7% uncertainty in the cross section measurement at 16 GeV/c P_T, and a 4.5% uncertainty at 100 GeV/c. The uncertainty in the cross section due to backscattered photons and electrons is 2% at 16 GeV/c and 7% at 100 GeV/c. The uncertainty in the η/π^0 ratio [1] leads to a cross section uncertainty of 2% at 16 GeV/c and 0.2% at 100 GeV/c.

The entire mix of background sources has been checked by a sample of events with the same photon cuts as the data, but the isolation cut slightly relaxed. This shows agreement with expectations within the uncertainty on ϵ_b quoted above. Finally, there are additional uncertainties due to luminosity (3.6%), cut efficiencies (4.8%), and photon energy scale (4.5%). The uncertainties in the profile method are much larger (30-70%), and are given in [1], but the two methods agree to within 5% from 16-30 GeV/c.

From the number of prompt photons in a bin of transverse momentum, along with the acceptance and the integrated luminosity for that bin, we obtain the isolated prompt photon cross section which is tabulated in Table 1. The bin sizes were chosen to maintain sufficient statistics to perform the background subtraction. As mentioned earlier, we have used the profile method for the first point from 10-16 GeV/c, and the conversion method for all other points. Also tabulated are the number of events, number of photons after background subtraction, statistical and systematic uncertainties. The systematic uncertainties listed are approximately 100% correlated and include all normalization uncertainties. The statistical and systematic uncertainties are significantly smaller than that of the previous best collider measurement [7].

In Fig. 3 our measurements from both 1989 and 1992 are compared to a next to leading order QCD calculation [8] derived using the CTEQ2M parton distributions [9] at a renormalization scale $\mu = P_T$. Inset is a comparison of the two background subtraction methods in their overlap region. The QCD prediction agrees qualitatively with the measurements over more than 4 orders of magnitude in cross section. Figure 4 shows on a linear scale that the QCD models have a slope that is less steep than the measured cross section at low P_T. Also shown is the prediction using CTEQ2ML [9] parton distributions which produces mostly a shift in normalization, and MRSD- [10] parton distributions which show little change. The QCD prediction changes by only 7% when the renormalization scale is doubled or halved, and both only give a normalization shift to the prediction. One possible cause of the difference between the data and the QCD calculation is the *bremsstrahlung* process [11], prevalent at low P_T, in which an initial or final state quark radiates a photon. QCD predictions show

good agreement with recent measurements of this process at LEP [12], however recent higher order calculations of this process [13] in $p\bar{p}$ collisions do indicate a slightly more steep prediction at low P_T. The remaining differences could indicate that for the first time we are measuring the gluon distribution inside the proton in a fractional momentum range where it has not been measured well before.

We thank the technical staffs of the participating institutions for their vital contributions. This work was supported by the U.S. DOE, NSF, Italian INFN, the Japanese MSCE, and the A.P. Sloan Foundation. We also wish to thank J. F. Owens for providing his computer code for the theoretical calculations.

References

[1] F. Abe *et al.* (CDF Collaboration). *Physical Review*, D(48):2998, 1993.

F. Abe *et al.* (CDF Collaboration). *Physical Review Letters*, 68:2734, 1992.

[2] J. Owens. *Reviews of Modern Physics*, 59:465, 1987.

[3] F. Abe *et al.* (CDF Collaboration). *Nuclear Instruments and Methods*, A(271):387, 1988.

[4] The event z vertex cut was relaxed to $|z| < 60cm$, and the missing transverse energy was required to be less than 80% of the photon transverse energy to remove cosmic rays.

[5] Y.S. Tsai. *Rev. Mod. Phys.*, 46:815, 1974.

[6] R. Brun *et al. GEANT3.* CERN DD/EE/84-1.

[7] J. Alitti *et al.* (UA2 collaboration). *Physics Letters*, B(263):544, 1991.

[8] J. Ohnemus, H. Baer and J.F. Owens. *Physical Review*, D(42):61, 1990.

[9] J. Botts *et al.* (CTEQ Collaboration). *Physics Letters*, B(304):159, 1993.

[10] A.D. Martin, W.J. Stirling, and R.G. Robert. *Physics Letters*, B(306):145, 1993.

[11] Edmond L. Berger and Jianwei Qiu. *Physical Review*, D(44):2002, 1991.

P. Aurenche *et al.* *Next to Leading Order Bremsstrahlung Contribution to Prompt-Photon Production*, May 1992. ENSLAPP-A-386/92.

[12] P.D. Acton *et al.* (OPAL Collaboration). *Zeitschrift fur Physik*, C(54):193, 1992.

O. Adriani *et al.* (L3 Collaboration). *Physics Letters*, B(292):472, 1992.

P. Abreu *et al.* (DELPHI Collaboration). *Zeitschrift fur Physik*, C(53):555, 1992.

D. Decamp *et al.* (ALEPH Collaboration). *Physics Letters*, B(264):476, 1991.

[13] M. Gluck *et al.* *High-p_T Photon Production at $p\bar{p}$ Colliders*, Feb. 1994. DO-TH 94/02.

P_T Bin (GeV/c)	P_T (GeV/c)	# Events	# Photons	$d^2\sigma/dP_T d\eta$ (pb/(GeV/c))	Stat. (%)	Sys. (%)
$10-16$	12.3	3982	897	4.46×10^3	9.3	16
$16-18$	17.0	30046	13943	1.30×10^3	2.9	12
$18-20$	19.0	28165	14675	8.05×10^2	2.6	11
$20-22$	21.0	17427	9064	4.58×10^2	3.3	10
$22-24$	23.0	10923	6033	3.08×10^2	3.8	10
$24-26$	25.0	7042	4362	2.26×10^2	4.3	10
$26-28$	27.0	4642	3118	1.63×10^2	4.9	10
$28-30$	29.0	3169	2012	1.06×10^2	6.1	10
$30-32$	31.0	2240	1433	7.67×10^1	7.2	9
$32-36$	33.9	2883	1974	5.37×10^1	6.0	9
$36-40$	37.9	1548	1110	3.09×10^1	7.9	9
$40-44$	41.9	942	722	2.05×10^1	9.5	9
$44-55$	48.9	1135	710	7.61×10^0	10.0	10
$55-72$	62.4	659	564	3.09×10^0	10.2	10
$72-92$	80.8	205	184	9.11×10^{-1}	17.4	10
$92-152$	114.7	95	90	1.63×10^{-1}	25.2	11

Table 1: The cross section calculated using the profile and conversion methods is tabulated along with the statistical and systematic uncertainties. The systematic uncertainties include normalization uncertainties and are $\approx 100\%$ correlated bin to bin.

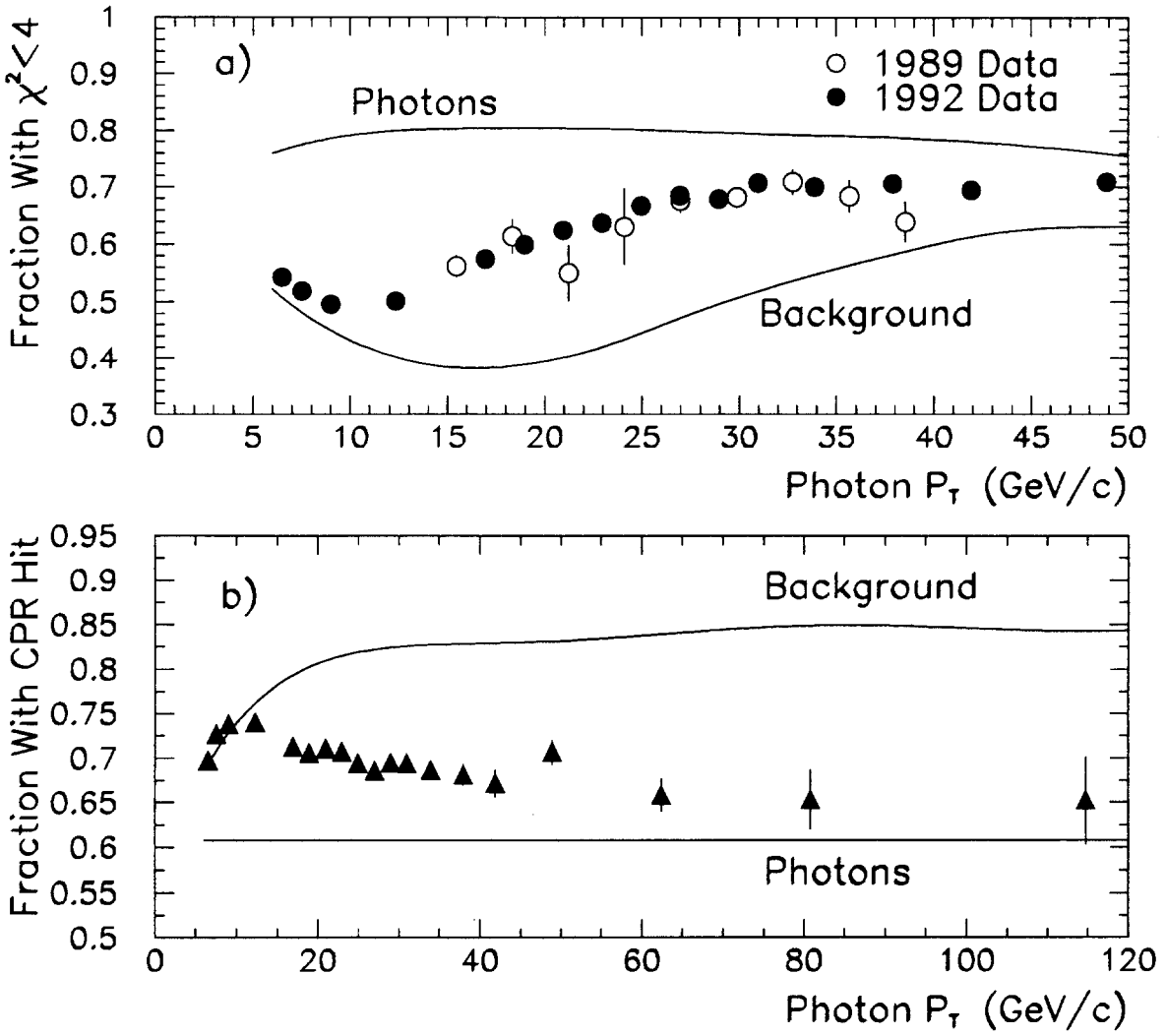

Figure 1: Illustration of the photon background subtraction methods. In a) is shown the profile method, with the fraction of photon candidates with $\tilde{\chi}^2 < 4$ (ϵ) along with the predictions for single photons (ϵ_γ) and background (ϵ_b). In b) the same is shown for the conversion method, with ϵ in this case being the fraction of photon candidates with a CPR signal.

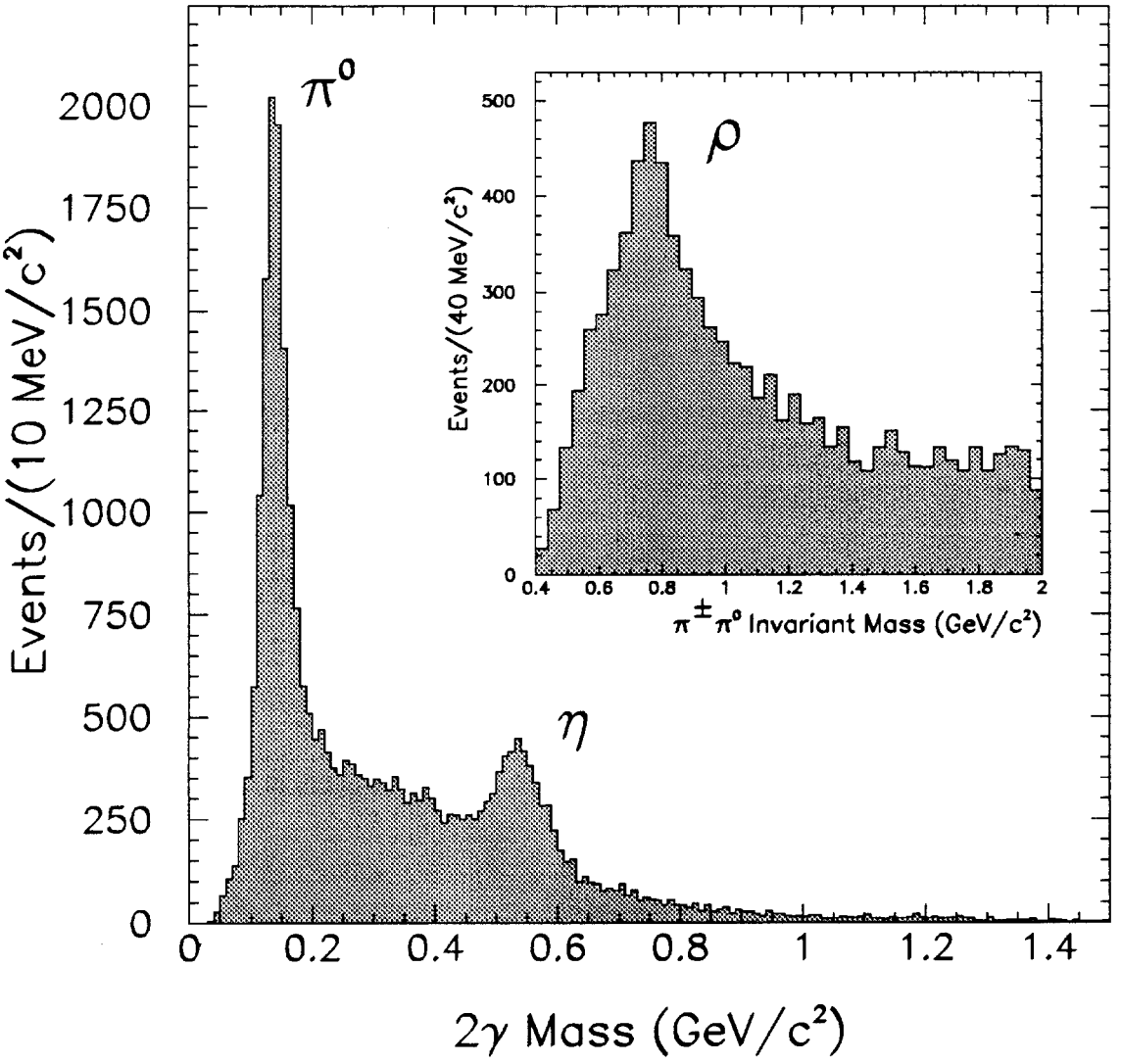

Figure 2: The 2 photon mass distribution, displaying reconstructed π^0 and η mesons. Inset is the reconstructed charged ρ meson peak. All three reconstructed mesons are used for the determination of the CPR conversion rate uncertainties.

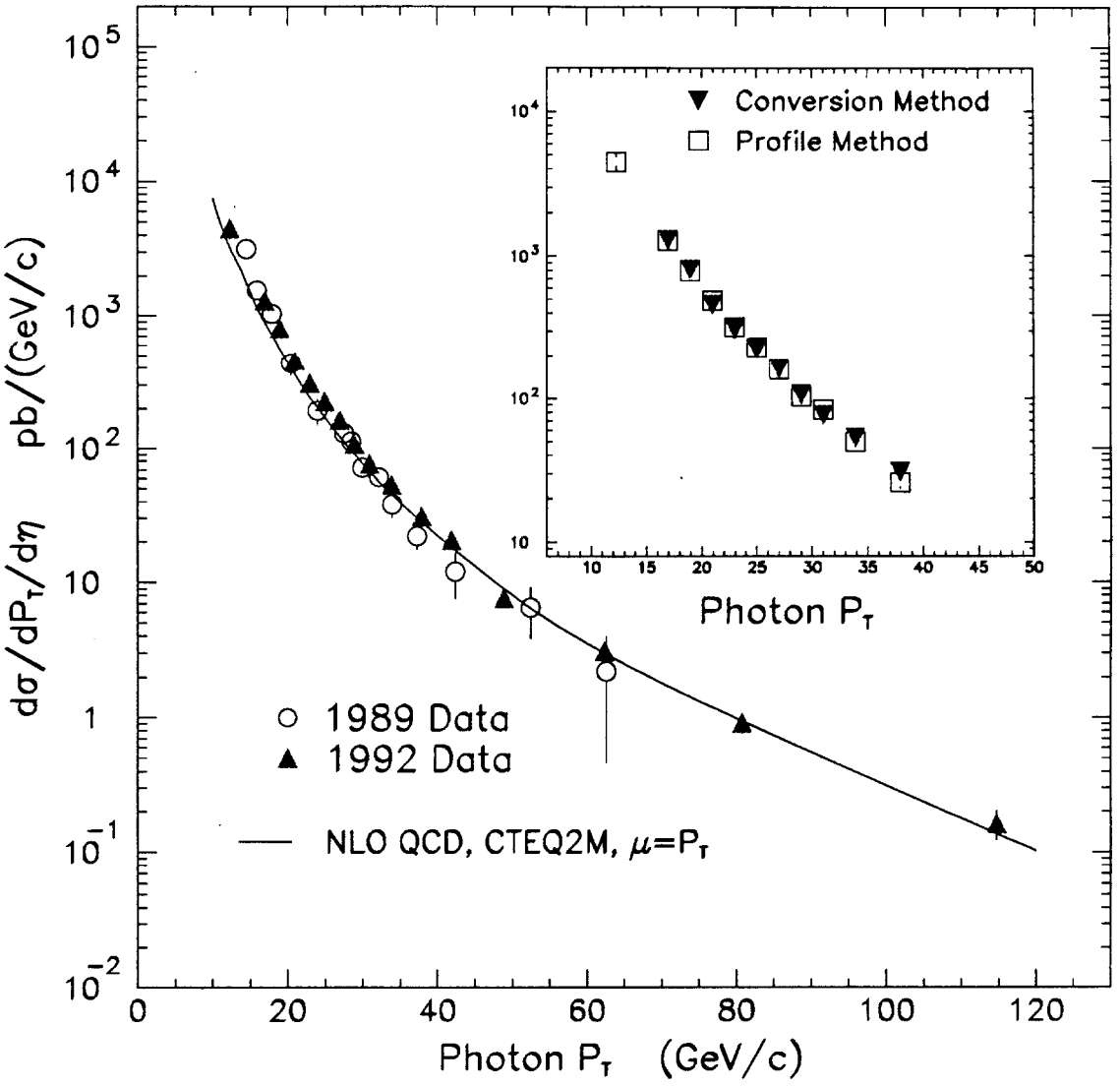

Figure 3: The inclusive isolated prompt photon cross section from 1989 and 1992 compared with a next-to-leading order QCD prediction. Inset is the comparison of the two background subtraction methods in their region of overlap.

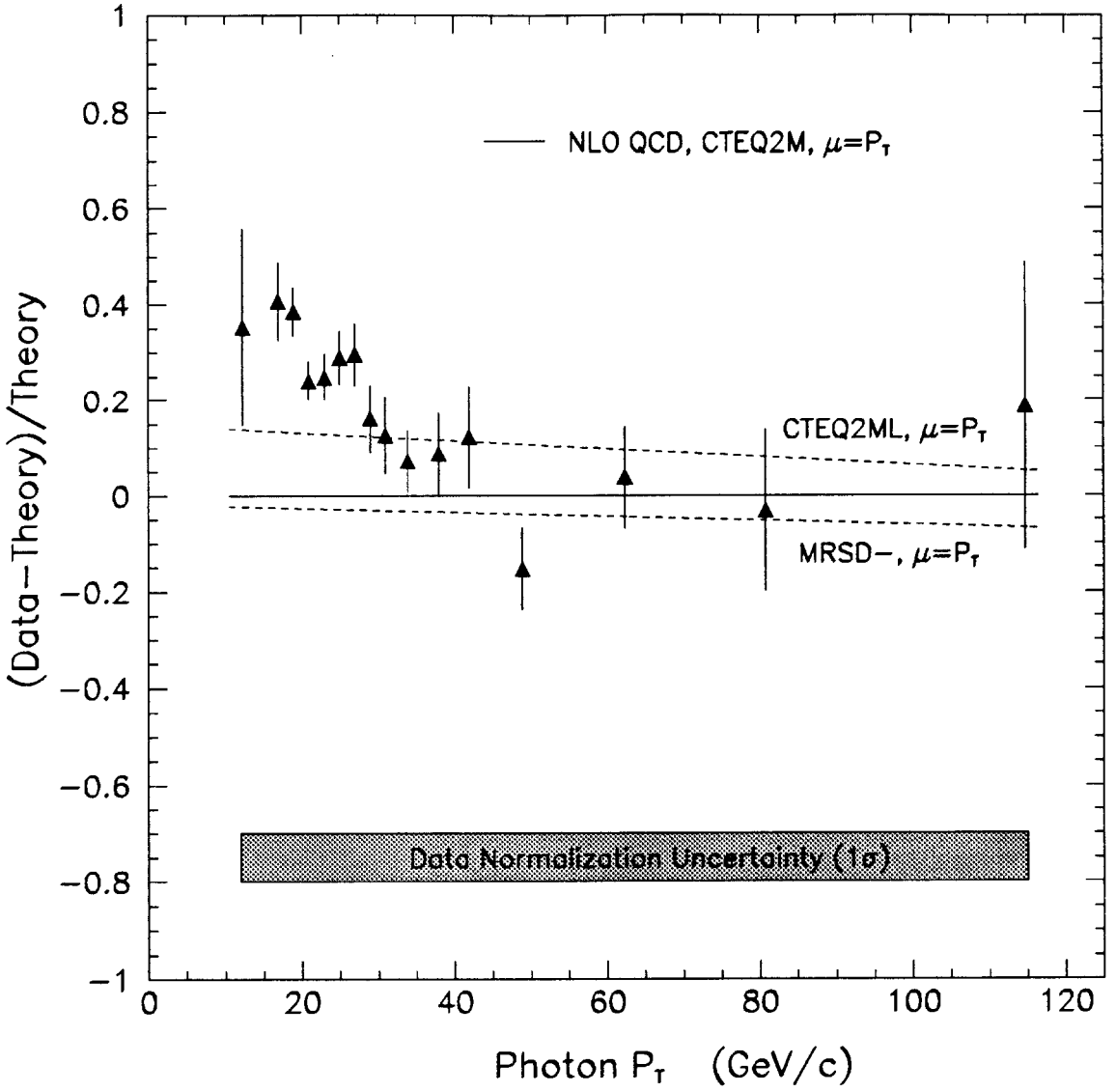

Figure 4: The prompt photon cross section measurement is compared with NLO QCD predictions and variations of parton distributions. At bottom is the data systematic uncertainty band, which is nearly 100% correlated point-to-point and includes normalization uncertainties.